Investigation of the anisotropy of electron–phonon interaction in zinc by the method of microcontact spectroscopy

I. K. Yanson and A. G. Batrak

Physicotechnical Institute of Low Temperatures, Ukrainian Academy of Sciences
(Submitted 14 July 1978)
Zh. Eksp. Teor. Fiz. **76**, 325–339 (January 1979)

Small deviations from Ohm's law in the conductivity of pressure point microcontacts of zinc were investigated at low temperatures. It was observed that the dependence of the second derivative of the current–voltage characteristic on the contact voltage differs significantly for single-crystal electrodes with different orientations. Inasmuch as, according to the theory, the second derivative is proportional to the transport function $G_n(\omega)$ of the electron–phonon interaction along the current-flow direction, the experimental data are compared with the anisotropic electron–phonon interaction functions $g_k(\omega)$ calculated by Truant and Carbotte, and also with the results of calculations of $G_n(\omega)$ for a simple model of the anisotropic phonon spectrum. Good qualitative agreement between theory and experiment is established. The electron–phonon interaction spectra corresponding to orientation of the contact axis along the c axis of the crystal are characterized by the presence of an intense low-frequency maximum in the region 7–8 meV. If the axis of the contact is inclined away from the direction of the c axis of the crystal toward the basal plane, the intensity of the low-frequency peak in the spectrum decreases substantially, while the intensity of the spectrum in the region of medium frequencies increases.

PACS numbers: 71.38. + i, 72.15.Eb

INTRODUCTION

The direct proportionality of the electron-phonon interaction function and the second derivative of the current–voltage characteristics of metallic microbridges was first noted for short-circuited metal–insulator–metal film contacts.[1] These relations, called the microcontact spectra, were measured for a number of metals and revealed good agreement between the positions of the singularities on the energy axis and the corresponding maxima of the phonon-state densities. Shortly after, Jansen, Mueller, and Wyder[2] have shown that similar relations can be obtained also with pressure contacts of the "needle–anvil" type between bulk metals. This procedure makes it possible in principle to investigate the anisotropy of the electron–phonon interaction in metals, if the electrodes of the contacts are made of single crystals of given orientation.

The theory of microcontact spectroscopy of metals[3-5] has confirmed the qualitative interpretation given in Ref. 1 for the observed phenomena. The dependence of the microcontact spectra on the crystallographic orientation arises when account is taken of the quasimomentum conservation law in the process of electron scattering by phonons and, according to Kulik, Omel'yanchuk, and Shekhter,[3] leads to the following dependence of the second derivative d^2I/dV^2 on the voltage V on the contact (as $T \to 0$):

$$\frac{d^2I}{dV^2}(V) = -4e^3N(0)\frac{d^3}{3}G(eV) = -\frac{2e^3N^2(0)}{3\hbar}d^3\left(\oint\frac{dS_{\mathbf{p}}}{v}\oint\frac{dS_{\mathbf{p}'}}{v'}\right)^{-1} \times\sum_s\oint\frac{dS_{\mathbf{p}}}{v}\oint\frac{dS_{\mathbf{p}'}}{v'}K(\mathbf{p},\mathbf{p}')w_{\mathbf{p}-\mathbf{p}',s}\delta(eV-\hbar\omega_{\mathbf{p}-\mathbf{p}',s}). \quad (1)$$

Here d is the diameter of the round opening in the infinitesimally thin partition that separates the two metals, $N(0)$ is the density of the electronic states on the Fermi surface [for free electrons with one spin projection we have $N(0) = mp_F/2\pi^2\hbar^3$]; $w_{\mathbf{p}-\mathbf{p}',s}$ is the square of the modulus of the matrix element of the electron–phonon interaction in scattering by a phonon with wave vector $\mathbf{q} = \mathbf{p} - \mathbf{p}'$ corresponding to the s-th branch of the phonon spectra $\omega_s(\mathbf{q})$. The integration in (1) is over the Fermi surfaces on which the ends of the electron quasimomentum lie before ($\mathbf{p}$) and after ($\mathbf{p}'$) the scattering. The characteristic (1) depends not only on the potential difference V, but also on the orientation of the contact symmetry axis Z passing through the center of the opening, perpendicular to the plane of the partition, relative to the crystallographic axes whose directions are assumed to coincide in both electrodes. The sensitivity to the sample orientation is determined by the factor $K(\mathbf{p},\mathbf{p}')$, which takes in the Kulik–Omel'yanchuk–Shekhter model the form

$$K(\mathbf{p},\mathbf{p}') = \frac{|p_zp_z'|}{|p_z\mathbf{p}'-p_z'\mathbf{p}|}\theta(-p_zp_z'). \quad (2)$$

The θ function is a reflection of the fact that the z-th component of the velocity must reverse sign in the scattering processes that are responsible for the observed nonlinearities of the current–voltage characteristic. It is easily seen that the directional selectivity of the method is relatively low in this model and reduces to a combination of trigonometric functions of the incidence and scattering angles under the integral sign in (1). One can nevertheless expect that in strongly anisotropic metals with one clearly pronounced crystallographic axis the microcontact spectra observed along this axis and in directions perpendicular to it will differ substantially. In this sense, a suitable object is zinc, for which we have investigated previously the microcontact spectra of the electron–phonon interaction, using samples in the form of polycrystalline films.[6] The observed anomalously large variations of the relative intensity and of the shape of the peaks in the microcontact spectra were interpreted as an indi-

 0038-5646/79/010166-08$02.40

rect indication of a strong anisotropy of the electron–phonon interaction in this metal, which manifests itself when the crystals are oriented at random at the point of contact.

In the present study we have obtained, for the first time ever, direct data on the anisotropy of the microcontact spectra of the electron–phonon interaction of single crystals with various orientations[1)] (preliminary results were published in Ref. 7). The choice of zinc as the object of the investigation was dictated not only by the considerations advanced above, but also by the fact that Truant and Carbotte[8] have carried out a detailed theoretical analysis of the anisotropy of the electron–phonon interaction in this metal. Notwithstanding the fact that the anisotropy functions of the electron–phonon interaction calculated by them $g_k(\omega) = \alpha_k^2(\omega)F_k(\omega)$ differ by definition from the transport functions $G_n(\omega) = \tilde{\alpha}_n^2(\omega)F_n(\omega)$ of the electron–phonon interaction registered by the method of microcontact spectroscopy, the main qualitative predictions made by them are confirmed by the results of our experiments. We next calculated for a simple model of an anisotropic phonon spectrum the microcontact spectra of the electron–phonon interaction in the case of orientation along the symmetry axis and perpendicular to it; these spectra illustrate clearly the experimentally observed tendencies. Finally, considerable attention was paid to the problem of the background, which was always present in experiment and which has so far not found a theoretical explanation. A comparison of the previously proposed various empirical methods for taking the background into account indicates that they are not satisfactory. In the present paper we propose a new method of subtracting the background, the main distinction of which is the closer connection with the observed microcontact spectra.

EXPERIMENTAL TECHNIQUE

Figure 1a shows the construction of the controlled point contact. In contrast to Ref. 2, we did not use a piezoceramic for precision regulation of the distance between the electrodes. The electrodes 1 were made of two single crystals *of identical orientation.* The plane of the anvil was usually a partially cleaved surface.

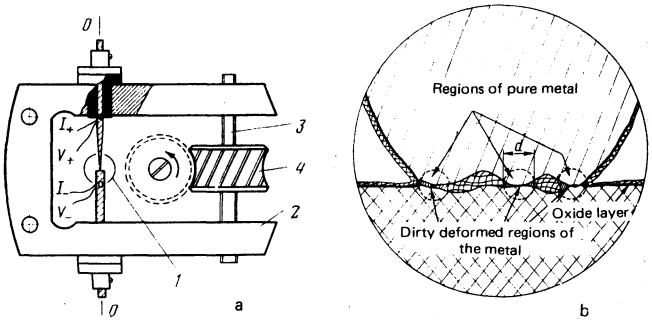

FIG. 1. a) Construction of regulated point contact: 1—single-crystal electrodes of identical orientation along the *OO* axis, 2—bracket, 3—differential screw, 4—worm gear. b) Schematic representation of cross section of the region of contact between the electrodes.

The needle was sharpened by chemical etching in HNO_3 and was electrically polished in H_3PO_4. The taper of the needle point was 40–50°, and at small angles the needle was seen to bend after contact with the anvil, causing an uncertainty in the orientation along the contact axis. Since the surfaces of the needle and of the anvil were covered with a thin layer of oxide during the time necessary to mount the sample on the holder, a high resistance (several dozens ohms) contact is produced when the two first touch lightly in liquid helium; this contact had a smeared out spectrum and a large background. It appears that the reason for this is that the diameter of the contact is small in this case, and therefore the interaction volume is also small ($\sim d^3$) and does not span the pure-metal regions in the interiors of the electrodes. With further increase of pressure on the contact, its effective diameter increases, and if this diameter becomes larger than the thickness of the layer of contaminated and deformed metal on the interface, then the interaction includes also the region of pure metal (Fig. 1b). It is thus possible to obtain information on the relatively "deep" pure layers of metal, and hence take into account also the anisotropy.

Such a contact can be approximately described by the model of Kulik, Omel'yanchuk, and Shekhter,[3] in which it is necessary to introduce a phenomenological factor T to account for the scattering of the electrons by the defects on the interface, in analogy with the procedure used by van Gelder.[4] It is possible to verify that in the microcontact-spectroscopy method the information comes not only from the boundary region but also from deeper layers of the metal by investigating the spectra of heterocontacts. As shown by Jansen, Mueller, and Wyder,[2] the spectra of Cu–Au heterocontacts are superpositions of the spectra of each metal separately. Similar results were obtained by us in the study of the spectra of Cu–Zn heterocontacts. It should also be noted that when the first contact is made between the electrodes one usually observes a spectrum, albeit a poor one, corresponding to the established orientation. When forces are subsequently applied to decrease the resistance and to increase the interaction region, an admixture of a spectrum with a different orientation can appear (if the needle bends or its end is cleaved off), or else a spectrum typical of polycrystalline film samples (in the case of excessive contamination of the contacting surfaces or "welding" of the contact by dielectric breakdown). The stable and reproducible results cited in the next section were therefore obtained with samples having the cleanest contacting surfaces (corresponding to the minimum interval of time between the electrode preparation and their installation in the cryostat).

The microcontacts satisfied the following "quality criteria," by following which we could select the spectra with "good" characteristics for their subsequent analysis and reduction.

1. The observed nonlinearity of the current–voltage characteristic must correspond to a metallic conductivity of the contact, i.e., the differential resistance of the contact increases with decreasing voltage on the contact. Usually the relative increase of dV/dI does not

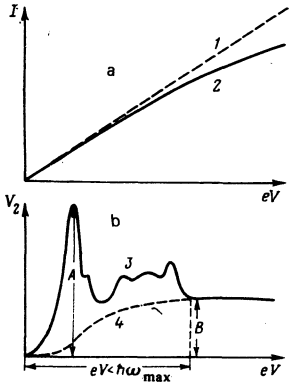

FIG. 2. Determination of the quality of the microcontacts: a) by the form of its current–voltage characteristics and b) from its second derivative (see the text). Curve 1—according to Ohm's law, 2—real I-V characteristic, deviation from Ohm's law greatly exaggerated; 3—dependence of the second-harmonic voltage of the modulating signal V_2, which is proportional to d^2V/dI^2, on the voltage in the sample; 4—assumed dependence of the background on the energy. The coefficient $\gamma = B/A$ characterizes the relative level of the background at $eV \geq \hbar\omega_{max}$.

exceed several percent. In a somewhat exaggerated form, the corresponding current–voltage characteristic is shown schematically in Fig. 2a.

2. The singularities (maxima, kinks, etc.) should be observed only in the voltage interval $0 < eV < \hbar\omega_{max}$, where $\hbar\omega_{max} \approx k\Theta_D$ is the maximum frequency of the phonon spectrum. At $eV > \hbar\omega_{max}$ only a smooth background should be observed (usually constant or weakly dependent on V). This is shown schematically in Fig. 2b. The absence of singularities at $eV > \hbar\omega_{max}$ means, in particular, that no contribution is made to the observed spectrum by excitations of molecular impurities whose localized vibrational modes have usually an energy higher than $k\Theta_D$.

3. The background level γ, defined as the ratio of the signal at $eV > \hbar\omega_{max}$ to the signal at the largest maximum of the spectrum, should be small enough ($\lesssim 0.5$).

All the measurements were made at a temperature 1.5 K using the standard modulation procedure of tunnel spectroscopy. The sensitivity in the channel of the second-harmonic signal V_2, proportional to the second derivative of the current–voltage characteristic, was ~10^{-8} V, and the modulating signal V_1 ranged from 0.1 to 0.4 mV.

Since the line-broadening mechanisms are the same in microcontact spectroscopy and inelastic tunneling, the resolution is determined in accordance with Refs. 9 and 10 by the formula

$$\delta(eV) = [(5.44kT)^2 + (1.22eV_1)^2]^{1/2}$$

and amounts in our experiments to 0.7–0.8 meV. It is due mainly to the temperature smearing of the electron distribution near the Fermi level.

The value of G function was determined from the formula

$$G = 0.546(V_2/V_1^2)d^{-1},$$

which follows from (1) in the free-electron model if it is recognized that $d^2I/dV^2 \approx (1/R_0)(4V_2/V_1^2)$, $N(0) = 3n/4\varepsilon_F$ and $v_F = 10^{-8}$ cm/sec. Here V_2 and V_1 are the effective values of the voltages of the second and first harmonics of the modulating signal (in microvolts and millivolts, respectively), and d is the contact diameter determined from the formula for the model of a clean opening (in nanometers):

$$d = \left(\frac{3\pi\rho l}{16R_0}\right)^{1/2} = \left(\frac{3042}{R_0(\Omega)}\right)^{1/2}. \quad (3)$$

The value of $\rho l = p_F/ne^2$ for zinc was assumed to be 1.8×10^{-11} $\Omega \cdot \text{cm}^2$ (n is the electron concentration); R_0 is the resistance of the contact at $V = 0$.

MEASUREMENT RESULTS

1. The orientation [0001]

We investigated the characteristics of several different pairs of "needle–anvil" electrodes oriented along the c axis. It was possible to carry out on each pair numerous measurement cycles, between which the electrodes were additionally purified and polished, and the needle was chemically sharpened. In each measurement cycle, by regulating the pressure between the electrodes, a number of different contact resistances is usually established and the corresponding microcontact spectra determined.

Figure 3 shows some of the microcontact spectra recorded with a two-coordinate potentiometer and one measurement cycle. The numbers next to the curves indicate the numbers of the spectra plotted in accordance with the table, in the same sequence in which the resistances of the contacts were established. It is seen from the table and from Fig. 3 that the resistance of the contact can be varied reversibly with the aid of the regulating screw by a factor of several times, with a negligible accompanying change of the shape of the spectrum (curves 1 and 8 in Fig. 3 correspond to approximately identical resistances). The other parameters that characterize the spectrum, such as the relative background level γ and the relative second-harmonic

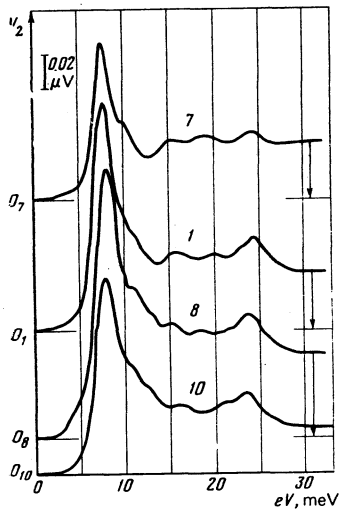

FIG. 3. Microcontact spectra of electron–phonon interaction along the [0001] axis. The number of the curve corresponds to the number of the contact in the table.

TABLE I. Successive changes of the resistances and of the parameters of the spectra in the course of regulation of the pressure on the pressure microcontact Zn [0001].

№	R_0, Ω	γ	V_2/V_1^2, per volt	G_{max}	V_1, mV	№	R_0, Ω	γ	V_2/V_1^2, per volt	G_{max}	V_1, mV
1	8.2	0.28	1.55	0.044	0.3	6	2.2	0.68	4.15	0.06	–
2	4.0	0.45	2.66	0.052	–	7	4.1	0.39	2.4	0.048	0.2
3	12.0	0.24	1.37	0.046	–	8	8.0	0.27	1.31	0.036	0.4
4	9.2	0.3	1.76	0.052	–	9	9.1	0.32	1.24	0.036	–
5	7.7	0.35	2.94	0.054	–	10	12.0	0.24	1.13	0.038	0.35

*V_1 and V_2 are the effective fundamental and secondharmonic voltages of the modulating signal.

voltage in the principal maximum of the spectrum, also have an approximately reversible behavior. The reversibility of the observed characteristics obviously means that the indicated limits of the change of the resistance correspond to elastic deformation of the metals in the region of the contact. It appears that the apparent discrete variation of the values of R_0 in the table is due to the insufficiently smooth regulation.

The spectra corresponding to orientation along the c axis are characterized by the presence of an intense low-frequency maximum in the region of 7–8 meV. The intensity of the spectrum in the region of medium energies is small. It increases somewhat if the resistance of the contact decreases jumpwise because of the electric breakdown or when the contact deformation exceeds the limits of the reversible variation of its properties. In these cases, the form of the spectrum comes close to that observed for short-circuited film samples in Ref. 6 (see also curve 1 in Fig. 10 below).

Just as in the investigation of film contacts of copper[11] and zinc,[6] single-crystal zinc exhibits a linear relation between the relative background level at $eV > \hbar\omega_{max}$ and $R_0^{-1/2}$. Figure 4a shows this function plotted against the contact diameter calculated by formula (3). A similar relation for polycrystalline pressure contacts of copper

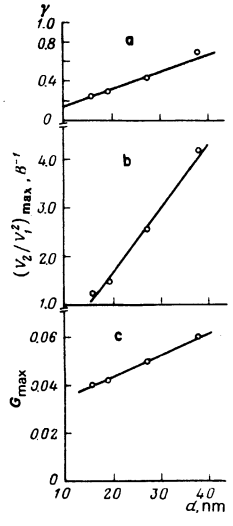

FIG. 4. a) Relative background level γ, b) the logarithmic derivative $d(\ln R_D)/dV = 4V_2/V_1^2$ of the differential resistance $R_D = dV/dI$, and c) the electron–phonon interaction function G at the principal maximum of the spectrum, vs the contact diamter d calculated from formula (3). Results—for the contact whose characteristics are given in the table and in Fig. 3.

was observed in Ref. 2. According to the theory,[3,4] in clean contacts the amplitude of the second-harmonic signal V_2 is proportional to $R_0^{-1/2}$, since the maximum value of the electron–phonon interaction function $G(\omega)$ should remain constant when the hole diameter is varied. It can be verified from Figs. 4b and 4c that these relations are approximately satisfied. It is seen that when V_2/V_1^2 is changed by a factor of four the value of G_{max} changes by a factor 1.5. We note that in dirty contacts the opposite picture is observed[5]: V_2/V_1^2 depends little on the resistance, whereas G_{max} calculated from formula (1) increases approximately in proportion to R_0. According to the theory of Ref. 5, the reason for this is that at $l_i < d$ the role of the characteristic length is transferred from the contact dimension d to the mean free path l_i due to scattering by impurities and defects. If the contacts are dirty, the relation between γ and $R_0^{-1/2}$ is likewise no longer linear in the experiment. Thus, the clamped point contact Zn [0001] considered above agrees satisfactorily with the model of a clean opening.

From the quantitative point of view, the values of G_{max} calculated from formula (1) are smaller by approximately one order of magnitude than the expected ones. The reason for this discrepancy is not quite clear. It is due in part to the choice of the theoretical model. In addition, such uncontrollable factors as a thin contamination layer on the interface between the two metals or the large number of short circuits can also be responsible for the lower experimental values of G_{max}.

For all the contacts with orientation [0001] investigated by us and satisfying the regularities noted above, the reproducibility of the spectrum was quite satisfactory. Conclusions concerning the possible variations of the form of the spectrum can be drawn from the curves shown in Fig. 3.

2. The orientation [11$\bar{2}$0]

When the contact axis is oriented along [11$\bar{2}$0] in the basal plane, the observed microcontact spectra are substantially different from those obtained along the c axis. Figure 5 shows the spectrum for one of the samples. The spectra are numbered in accordance with the sequence of the variation of the contact resistance. The main difference from the microcontact spectra obtained along the c axis lies in the larger relative intensity of the bands in the central part of the spectrum. The low-frequency maximum is shifted somewhat (8–9 meV) towards higher energies, and a similar systematic shift can be noted also for the high-frequency maximum, although it is masked by random variations of the position of this maximum on the energy axis (≈25 MeV). The sharp decrease of the contact resistance (to $R_0 = 0.78$ Ω) causes the microcontact spectrum to consist almost completely of the background ($\gamma > 1$; curve 4 on Fig. 5), and coincides approximately with the spectra having a low background level only on the initial section, before the first maximum. When the resistance of the contact is changed by several times (10 – 33.8 Ω) the form of the spectrum does not change qualitatively. Quantita-

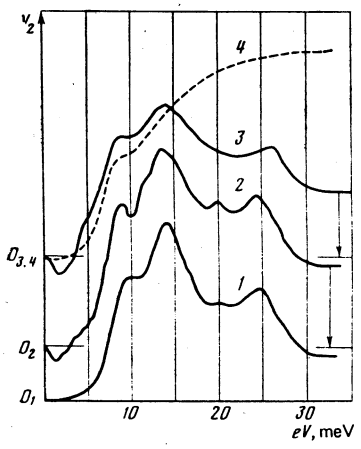

FIG. 5. Microcontact spectra of electron–phonon interaction along the [1120] axis. The sequence of the numbers of the curves corresponds to the sequence in the variation of the resistance: for curves 1–4 the resistances are 10, 12.7, 33.8, and 0.78 Ω; the effective values of the modulating voltage are 0.5, 0.5, 0.8, and 0.3 mV.

tively, the value of the G function calculated from formula (1) for the largest maximum of the spectrum (≈14 meV) is smaller by a factor 2 or 3 than G_{max} in the spectra for the orientation [0001].

The possible variations of the form of the spectra obtained along the [11$\bar{2}$0] axis with different pairs of electrodes are shown in Fig. 6. The most typical deviations from the "unpertrubed" spectra (curve 1) consists of an increase of the intensity of the low-frequency maximum, accompanied by its shift towards lower energies. The perturbations due to excessive deformation of the contact in the course of the measurements usually lead to a gradual transition to the form of the spectrum typical of polycrystalline film samples (see curve 1 on Fig. 10 below).

3. Background

Practically all the measured microcontact spectra contain a monotonically increasing background which saturates, as a rule, at $eV>\hbar\omega_{max}$ (Fig. 2b). A spectrum without a background can be obtained for shorted film contacts with extremely high resistance (≳100 Ω).[6,9] Such large values of the resistance and corresponding small diameters can usually not be obtained with pressure contacts. These contacts, however, can be made of electrodes of high purity, and this leads to a substantial decrease of the relative background level compared with film contacts having the same resistance. Since it is extremely difficult to obtain experimental spectra without a background, the problem arises of taking correct account of this background.

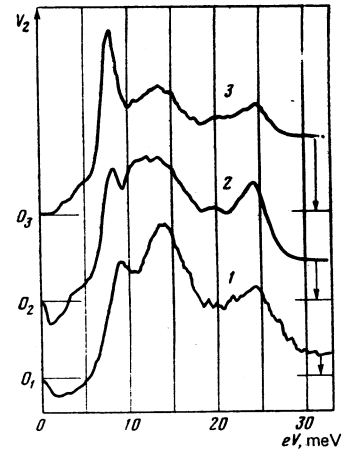

FIG. 6. Observed values of the spectra for different pairs of zinc electrodes oriented along the [11$\bar{2}$0] axis. The resistances are: 1—9.8Ω, 2—0.53Ω, 3—4.33Ω.

Initially Jansen, Mueller, and Wyder[2] proposed for the background the empirical formula

$$B(V)=C\,\mathrm{th}^2\,(1.5eV/k\Theta_D),$$

which was made to coincide with the observed spectrum at $eV>\hbar\omega_{max}$ by adjusting the constant C and the Debye temperature Θ_D. This function does not depend on the concrete form of the electron–phonon interaction function and is the same for all metals with equal values of Θ_D. To connect more closely the dependence of the background on the energy with the characteristics of the investigated metal, it was proposed in Ref. 6 to choose as the background the microcontact spectra with $\gamma>1$, which consist at sufficiently high values of eV of practically only the background. A typical example of such a spectrum is shown by curve 4 of Fig. 5 for a single-crystal contact with orientation [11$\bar{2}$0]. For polycrystalline contacts a background of this kind is shown in Fig. 7 (curve 4). In this case, however, we encountered the difficulty of taking into account the background on the initial section of the spectrum, where the background assumed by this method was substantially overestimated. It must be emphasized here that in the experiment the initial section of the spectrum (before the first maximum) is the same for all contacts of a given type, subject to a suitable choice of the scale factor on the V_2 axis, regardless of the value of γ. Consequently, the background level is small at small eV. It is obvious that the dependence of the background on eV is closely connected with the concrete form of the microcontact spectrum of the given contact, which was not taken into

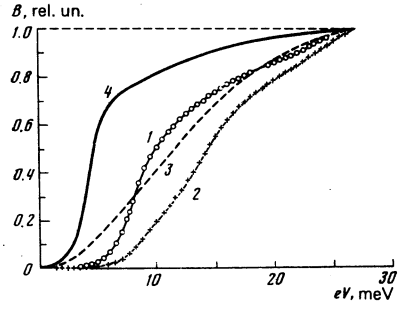

FIG. 7. Different dependences of the background on the energy: curves 1 and 2—in accord with the formula

$$B(V)=C\int_0^V G_0(V')\,dV',$$

for the orientations [0001] and [1120], respectively (see the text); curve 3—in accordance with the formula

$$B(V)=C\,\mathrm{th}^2(1.5eV/k\Theta_D)$$

in accord with Ref. 2; curve 4—spectrum of film zinc contact with $\gamma>1$ (Ref. 6).

account in the above-described empirical methods of allowing for the background.

Van Gelder[4] attempted to determine the background theoretically, taking two-phonon processes into account. The function obtained by him, however, does not saturate at $eV > \hbar\omega_{max}$ and is equal to zero at $eV > 2\hbar\omega_{max}$, in contradiction to the experimental data.

Since γ is proportional to d/l, it is reasonable to assume that the background $B(eV)$ is proportional to a quantity that depends on eV:

$$B(eV) \propto \frac{1}{l(eV)} \approx \frac{2\pi}{\hbar v_F} \int_0^{eV} G_0(\omega)\, d\omega; \qquad (4)$$

where G_0 is taken to mean the microcontact spectrum with the background subtracted. Formula (4) was written in analogy with the known relation for the electron–phonon mean free path (at $T = 0$):

$$1/l(\varepsilon) = (2\pi/\hbar v_F) \int_0^{\varepsilon} g(\omega)\, d\omega.$$

Thus, the background is determined from the equation

$$B(eV) = C \int_0^{eV} [V_2(\varepsilon) - B(\varepsilon)]\, d\varepsilon. \qquad (5)$$

The background calculated by formula (5) for the spectra corresponding to the orientations [0001] and [11$\bar{2}$0] is shown in Fig. 7 (curves 1 and 2, respectively). Being likewise empirical in essence, it is free of certain shortcomings of the approaches mentioned above.

4. COMPARISON WITH THEORY

1. Anisotropy of G functions for an axially symmetrical model of the phonon spectrum

Since a direct calculation of the G functions in different crystallographic directions by formula (1) is an exceedingly complicated task, it is useful to consider a simplified Debye model of the anisotropic phonon spectrum, with the aid of which it is possible to establish the qualitative tendencies of the variation of the form of G functions in contacts with different orientations. We assume the frequency of a phonon with given wave vector $\mathbf{q}$ to have the following dependence on the angle θ between this vector and the crystal axis $\mathbf{n}$

$$\omega(\mathbf{q}) = q\omega_0(\theta), \quad \omega_0(\theta) = \omega_0(1 + \sin\theta). \qquad (6)$$

This dispersion law corresponds approximately to the LA branch of the phonon spectrum of zinc, in which $\omega_q \propto q$, and the speed of sound along the c axis is approximately half the speed of sound in a direction perpendicular to it. We substitute (6) in (1) and calculate (by the Monte Carlo method with a computer) the functions $G_\perp$ and $G_\parallel$ corresponding to orientation of the crystal axis perpendicular or parallel to the separation plane that contains the contact opening. The results are shown in Fig. 8. In the calculations it was assumed that $p_F = q_D = 1$ and $w(q) = \text{const} \cdot \omega(q)$.

We verify first that the presence of the kernel (2) under the integral in (1) does indeed make it possible to register distinctly the anisotropy of the phonon spectrum. As might be expected,[7] the position of the maximum on the energy axis correlates qualitatively with the limiting energies of the phonons propagating along the symmetry axis of the contact; this axis passes through the center of the opening and is perpendicular to the separation plane. We now compare the results obtained for the model with the experimental zinc spectra plotted along the c axis (Fig. 3) and in the perpendicular direction (Fig. 5). The maximum energy of the phonons propagating along the c axis in zinc is $\approx$19 meV (LO branch), whereas for the phonons whose wave vectors lie in the basal plane we have $\hbar\omega_{max} = 25$–26 MeV (LA, LO, and $TO_\parallel$ branches).[12] Consequently one can expect the high-frequency maximum in the microcontact spectrum obtained along the c axis, corresponding to the G function, to be shifted towards lower energies compared with the position of the high-frequency maximum in the spectrum taken in the basal plane. The experimental data (Fig. 9b) agree with this conclusion.

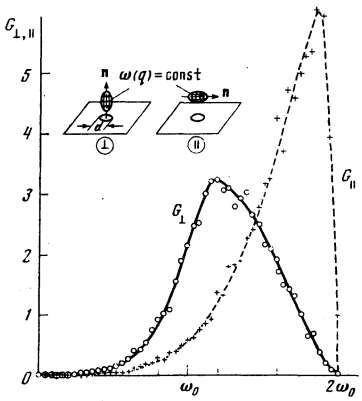

FIG. 8. Anisotropic electron–phonon interaction transport functions $G_\perp$ and $G_\parallel$, which are proportional to the microcontact spectra, calculated for the model phonon spectrum. The ordinates for both curves are given in unequal arbitrary units. The inset shows the orientations of the equal-energy surfaces of the phonons relative to the plane of contact for the two considered cases.

Analyzing the dispersion curves $\omega_s(\mathbf{q})$ for zinc[12] we

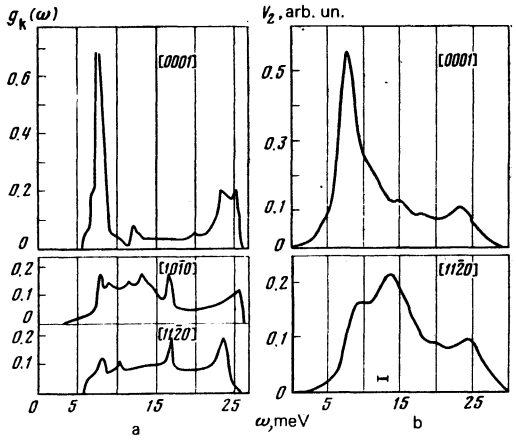

FIG. 9. Comparison of the anisotropic electron–phonon interaction functions $g_k(\omega) = \alpha_k^2(\omega)F_k(\omega)$, calculated by Truant and Carbotte[8] (a) with the microcontact spectra of zinc V_2(eV) $\propto G_0$(eV) along the c axis and in the basal plane (b). The background has been subtracted from the experimental curves.

can see that a large phonon state density is observed in the region ≈14–15 meV only for phonons propagating in the basal plane (the branches $TO_{\parallel}$ and $TA_{\parallel}$ along the $[10\bar{1}0]$ direction which is close to the $[11\bar{2}0]$ direction in which the measurements were made). This explains the presence of an intense maximum at $eV \approx 14$ meV in the microcontact spectra plotted along $[11\bar{2}0]$. A more detailed comparison of the theory with experiment within the framework of the simplified model assumed above cannot be carried out. For this purpose it is necessary to resort to a theory that takes into account the complex structure of the real phonon spectrum in zinc.

2. Comparison with the anisotropic functions $g_{\mathbf{k}}(\omega) = \alpha_{\mathbf{k}}^2(\omega)F_{\mathbf{k}}(\omega)$ of the electron–phonon interaction

Using the approximation wherein the electrons have a quadratic dispersion and the Fermi surface is spherical, but retaining without change the anisotropy of the real phonon spectrum, Truant and Carbotte[8] calculated the anisotropic electron–phonon interaction functions of zinc:

$$g_{\mathbf{k}}(\omega)=\alpha_{\mathbf{k}}^2(\omega)F_{\mathbf{k}}(\omega)=N(0)\int_{\Pi\Phi}\frac{d\Omega_{\mathbf{k}'}}{4\pi}\sum_{s}w_{\mathbf{k},\mathbf{k}',s}\delta(\omega-\omega_{\mathbf{k}-\mathbf{k}',s}) \qquad (7)$$

which are obtained when $K(\mathbf{p},\mathbf{p}')$ in (1) is replaced by a delta-function angle between the axis of the contact and the direction of the velocity of the electron incident on the opening. Naturally, this replacement simulates with great exaggeration the relatively weak dependence of the kernel $K_{\mathbf{p},\mathbf{p}'}$ on the angle $\eta[p_z=p\cos\eta$ in (2)]. It is nevertheless of interest to compare the $g_{\mathbf{k}}$ functions along the c axis and in the perpendicular direction with the corresponding microcontact spectra $G_{\perp}$ and $G_{\parallel}$. Such a comparison is shown in Fig. 9. The results of Truant and Carbotte are given for one of the two models they used for the force constants of the zinc lattice proposed by de Wames, Wolfram, and Lehman,[13] inasmuch as this model leads to better agreement between the energy position of the intense high-frequency peak for the function $g_{[0001]}$ (Fig. 9a) and the microcontact spectrum $G_{[0001]}$ (Fig. 9b). Generally speaking, the data of Truant and Carbotte should be represented in the form of a convolution with the resolution function of our spectrometer. This would lead to some smoothing and broadening [with increasing resolution $\delta(eV)$] of the sharp peaks on Fig. 9a, without changing their positions on the energy axis and without changing their relative intensities. Since our comparison is qualitative because the functions $g_{\mathbf{k}}(\omega)$ differ, by definition, from the microcontact spectra $G_{\mathbf{n}}(\omega)$, introduction of the foregoing small corrections is of no principal significance.

Figure 9a shows the functions $g_{\mathbf{k}}$ for two independent orientations in the basal plane. Since these orientations are close (the angle between them is 30°), the experimental microcontact spectrum in the $[11\bar{2}0]$ direction is in fact the result of their averaging, since directivity of the method corresponds to a 45° angle.[2] The experimental spectra are shown in Fig. 9b with the background subtracted in accordance with formula (5). On the whole, the agreement between the anisotropic $g_{\mathbf{k}}$ functions and the microcontact spectra $V_2(eV)$, which are

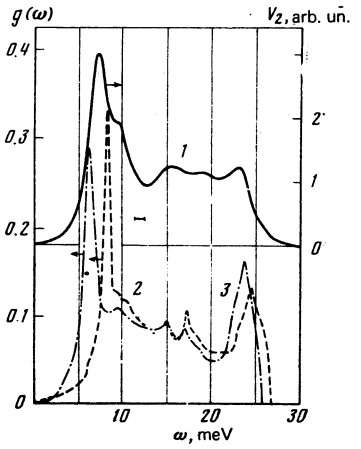

FIG. 10. Comparison of the microcontact spectra of polycrystalline zinc (curve 1) with the isotropic functions of the electron–phonon interaction $g(\omega)$ (curves 2 and 3) calculated in Ref. 8 and corresponding to different systems of force constants simulating the real phonon spectrum.

proportional to the $G_{\mathbf{n}}$ functions, is much better than expected. The main result of the theory of Ref. 8, shown in Fig. 9a, is that if the vector $\mathbf{k}$ is deflected away from the direction along the c axis towards the basal plane, then the intensity of the low-frequency peak decreases substantially, while the intensity of the spectrum in the region of medium frequencies increases. Experiment (Fig. 9b) confirms this prediction. In Fig. 9b, the V_2 scales are shown in arbitrary units that are the same for both orientations. Consequently, the relative intensity of the experimental spectra obtained in mutually perpendicular directions are also in good agreement with the theory (Fig. 9a).

Finally, Fig. 10 shows for the sake of completeness a comparison of the microcontact spectrum of polycrystalline zinc, obtained with film contacts, with the isotropic functions of the electron–phonon interaction

$$g(\omega)=\alpha^2(\omega)F(\omega)=\int_{FS}\frac{d\Omega_{\mathbf{k}}}{4\pi}g_{\mathbf{k}}(\omega), \qquad (8)$$

which were also calculated by Truant and Carbotte[8] for two different models of the force constants. As already noted above, a spectrum similar to that shown by curve 1 of Fig. 10 is observed also in the case of considerable deformation of pressure contacts made of bulky electrodes. Both the theoretical functions $g(\omega)$ and the experimental direction-averaged spectrum $\langle G_{\mathbf{n}}(\omega)\rangle$, which is proportional to $V_2(eV)$ on Fig. 10, can be represented very roughly in the form of a superposition of anisotropic spectra taken in mutually perpendicular directions. Thus, the anisotropic microcontact spectra of the electron–phonon interaction in zinc, obtained in the present study, agree well with the earlier results for polycrystalline samples.[6]

CONCLUSION

The simplicity of the experimental procedure and the direct character of the obtained unique information on the electron–phonon interaction in metals are undisputed advantages of microcontact spectroscopy. One

must not lose sight, however, of the difficulties encountered when it comes to complete realization of these advantages. These include above all the need for producing contacts with controllable structure and geometry. Taking into account the extreme smallness of the dimensions (dozens or hundreds of Angstroms), this turns out to be a complicated experimental problem. The analogous problem in tunnel spectroscopy is the production of a thin (~20 Å) barrier layer of a dielectric with controllable properties.

Among the unsolved theoretical questions, notice should be taken of the need for correct allowance for the background, and also for a consistent analysis of the influence of impurities and defects in the contact region. The theory of microcontact spectroscopy in the dirty limit for several simple models was considered in Ref. 5. The main conclusion that follows from this work is the weak sensitivity of the method to the ratio of the impurity mean free path l_i and the contact dimension d, under the condition that the latter remains smaller than the energy relaxation length $\lambda = (l_i l_e)^{1/2}$ (l_e is the mean free path of the electron relative to inelastic relaxation processes). This makes it possible in principle to study the electron–phonon interaction in alloys and in amorphous semiconductors. If, however, $l_i \lesssim 2\pi/q$ (q is the wave vector of the phonon), then according to Ref. 14 the electron–phonon interaction function $g(\omega) = \alpha^2(\omega)F(\omega)$ undergoes substantial changes. It is possible that the noticeable decrease of the intensity of the bands in the high-frequency part of the microcontact spectra, which is frequently observed for dirty contacts, as well as the discrepancy between theory[3] and experiment[15] at low energies, are due precisely to this effect. Finally, it appears that one cannot neglect also the disequilibrium of the phonon subsystem in the case when the diameter of the contact is comparable with the phonon-electron scattering length. In this case the electrons can reabsorb phonons and this leads to an apparent increase of the energy relaxation length λ. It is known[16] that similar processes interfere seriously in measurements of the recombination time of quasiparticles in superconductors.

The authors are deeply grateful to I. O. Kulik for numerous useful discussions and to V. M. Kirzhner for help with the calculation of the anisotropic models of the G functions.

[1)] The first attempts to observe the anisotropy of electron–phonon interaction by the microcontact spectroscopy method were unsuccessful.[2] The negative result was apparently due to the fact that, of the two electrodes, only the anvil was a single crystal. In addition, owing to the high degree of symmetry of the copper lattice,[2] the anisotropy of the microcontact spectra should be low.

[1]I. K. Yanson, Zh. Eksp. Teor. Fiz. **66**, 1035 (1974) [Sov. Phys. JETP **39**, 506 (1974)]; Proc. Fourteenth Internat. Conf. on Low Temp. Phys., Vol. 3, Helsinki, 1975, pp. 506–509.
[2]A. G. M. Jansen, F. M. Mueller, and P. Wyder, Conf. on d- and f-superconductors, ed. D. H. Douglass, Amer. Inst. Phys. 1976, pp. 607–623; Phys. Rev. B **16**, 1325 (1977).
[3]I. O. Kulik, A. N. Omel'yanchuk, and R. I. Shekhter, Fiz. Nizk. Temp. **3**, 1543 (1977) [Sov. J. Low Temp. Phys. **3**, 740 (1977)]; Solid State Commun. **23**, 301 (1977).
[4]A. P. van Gelder, Solid State Commun. **25**, 1097 (1978).
[5]I. O. Kulik and I. K. Yanson, Fiz. Nizk. Temp. **4**, 1267 (1978) [Sov. J. Low Temp. Phys. **4**, 596 (1978)].
[6]I. K. Yanson, Fiz. Nizk. Temp. **3**, 1516 (1977) [Sov. J. Low Temp. Phys. **3**, 726 (1977)].
[7]I. K. Yanson and A. G. Batrak, Pis'ma Zh. Eksp. Teor. Fiz. **27**, 212 (1978) [JETP Lett. **27**, 197 (1978)].
[8]P. T. Truant and J. P. Carbotte, Can. J. Phys. **51**, 922 (1973).
[9]J. Klein, A. Léger, M. Belin, and D. Défourneu, Phys. Rev. B **7**, 2336 (1973).
[10]R. J. Jennings and J. R. Merrill, J. Phys. Chem. Solids **33**, 1261 (1972).
[11]I. K. Yanson and Yu. N. Shalov, Zh. Eksp. Teor. Fiz. **71**, 286 (1976) [Sov. Phys. JETP **44**, 148 (1976)].
[12]N. J. Chesser and J. D. Axe, Phys. Rev. B **9**, 4060 (1974).
[13]R. E. DeWames, T. Wolfram, and G. W. Lehman, Phys. Rev. **138**, A717 (1965).
[14]B. Keck and A. Schmid, J. Low Temp. Phys. **24**, 611 (1976).
[15]I. K. Yanson, Fiz. Tverd. Tela (Leningrad) **16**, 3595 (1974) [Sov. Phys. Solid State **16**, 2337 (1975)].
[16]D. N. Langenberg, Fourteenth Internat. Conf. on Low Temp. Phys., Otaniemi, Finland, Vol. 5, ed. Matti Krusius and Matti Vuorio, 1975, pp. 223–263.

Translated by J. G. Adashko